Carbohydrate Polymers 86 (2011) 462–468

Contents lists available at ScienceDirect

Carbohydrate Polymers

journal homepage: www.elsevier.com/locate/carbpol

Physical properties of silk fibroin/cellulose blend films regenerated from the hydrophilic ionic liquid

Songmin Shang*, Lei Zhu, Jintu Fan

Institute of Textiles and Clothing, The Hong Kong Polytechnic University, Hung Hom, Kowloon, Hong Kong, PR China

ARTICLE INFO

Article history:
Received 24 November 2010
Received in revised form 12 March 2011
Accepted 25 April 2011
Available online 5 May 2011

Keywords:
Silk fibroin
Cellulose
Blend film
Ionic liquid

ABSTRACT

In this work, silk fibroin/cellulose (SF/CE) blend films were regenerated from hydrophilic ionic liquid, 1-butyl-3-methylimidazolium chloride (BmimCl). The structure of the blend films was characterised by Fourier transform infrared spectroscopy (FTIR). The thermal and mechanical properties and the surface morphology of the blend films were also investigated. In addition, moisture content, swelling index, total water absorption and film weight loss were measured. The results indicate that with the introduction of CE, the interactions between SF and CE in the blend films induced the conformation transition of SF from random coil form or silk I to β-sheet structure. At the same time, the physical properties of the blend films were improved. When the ratio of SF to CE is 25:75, the stronger interactions in the matrices contribute to the higher tensile strength, higher thermal stability and higher water stability. However, the blend film with half CE illustrates higher elongation at break, a more homogeneous surface and higher miscibility.

1. Introduction

In recent years, increasing environmental and energy problems have promoted the development of renewable resources, including the large-scale production of biofuels and the replacement of natural polymers with petroleum-derived synthetic polymers (Atsumi, Hanai, & Liao, 2008; Li et al., 2009; Ma & Yu, 2004; Rubin, 2008). Among the diverse renewable resources, natural proteins and natural carbohydrates have attracted much attention.

Silk fibroin (SF), a fibrous protein, has been widely used not only in the traditional textile field but in the biomedical and biotechnological fields (Kaplan, Adams, Farmer, & Viney, 1994). In general, SF can be prepared for different morphologies, such as particles, fibres, films, sponges, hydrogels and scaffolds (Vepari & Kaplan, 2007). Among such morphologies, SF films have been extensively studied for the applications in tissue engineering (Lawrence, Marchant, Pindrus, Omenetto, & Kaplan, 2009; Wang, Kim, Novakovic, & Kaplan, 2006), enzyme immobilisation (Lu et al., 2009; Zhang, 1998), cell culture (Gupta et al., 2007) due to their excellent biocompatibility, biodegradable properties, relatively easy preparation technique and controllable process conditions (Lawrence, Omenetto, Chui, & Kaplan, 2008). Nevertheless, SF membranes have exhibited weak mechanical properties due to their brittle properties in the dry state, which limits their practical applications (Kweon, Ha, Um, & Park, 2001; Niamsa, Srisuwan, Baimark, Phinyocheep, & Kittipoom, 2009). Hence, many studies have been made to improve the physical properties of SF film by blending it with other polymers, such as polyvinyl alcohol (PVA) (Li, Minoura, Dai, & Zhang, 2001) and chitosan (Niamsa et al., 2009).

Cellulose (CE), a common carbohydrate, is one of the most abundant natural polysaccharides, exhibiting wide commercial applications in the field of textiles, papers, membranes, polymers and paints fields (Swatloski, Spear, Holbrey, & Rogers, 2002). In addition, CE can be designed and processed for the functional composites or blends, including CE/carbon nanotube composite fibres, CE/chitosan nanocomposite films, CE/PVA nanocomposite films and CE/corn protein blend films (Fernandes et al., 2009; Lu, Wang, & Drzal, 2008; Yang et al., 2009; Zhang et al., 2007). It is reported that the mechanical properties of the CE/corn protein blends can be improved due to strong hydrogen bonding between the hydroxy groups of CE and the hydroxy groups and amino groups of corn protein (Yang et al., 2009).

Hence, it would be an effective and promising method to improve the mechanical properties of SF and to broaden the potential of CE as a biomedical material candidate. Simultaneously, selection of SF and CE as model macromolecules would be beneficial in further investigating the interactions between proteins and polysaccharides.

Previously, there have been numerous studies reporting blend films prepared from SF and CE (Freddi, Romano, Massafra, & Tsukada, 1995; Yang, Zhang, & Liu, 2000). Freddi et al. first reported the preparation of SF/CE blend films using cuoxam solution, however, drawbacks of this method included environmental concerns, such as undesirable metal complex waste solution and the difficulties in removing Cu from the regenerated material. Recently, the organic cyclic amine oxide N-methyl morpholine N-oxide (MMNO)

* Corresponding author. Tel.: +852 69793168; fax: +852 27731432.
E-mail address: tcshang@inet.polyu.edu.hk (S. Shang).

0144-8617/$ – see front matter © 2011 Elsevier Ltd. All rights reserved.
doi:10.1016/j.carbpol.2011.04.064

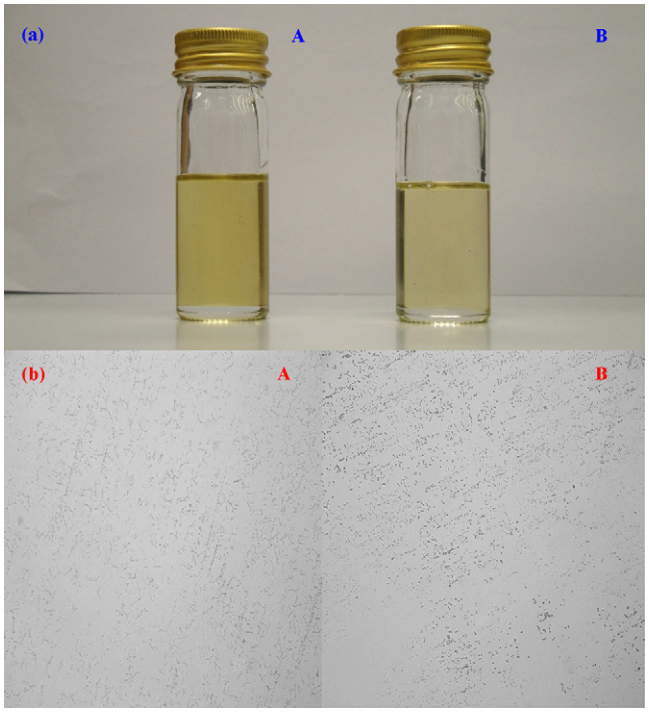

Fig. 1. Photographs (a) and microscopic photos (b) of SF-BmimCl solution (A) and CE-BmimCl solution (B). Magnification: 100×.

appeared to be an attractive reagent for preparing SF/CE blend films (Freddi, Pessina, & Tsukadab, 1999). Nonetheless, the water-sensitive MMNO made it necessary to conduct the reaction process under inert atmosphere, which is not a simple method. As a result, many researchers have searched for easier methods to prepare SF/CE blend films.

More recently, ionic liquids as green solvents, have attracted much attention due to their chemical and thermal stability, non-flammability and immeasurably low vapour pressure (Zhu et al., 2006). Rogers et al. (Swatloski et al., 2002) first reported the solubility of CE in ionic liquids and analysed the corresponding dissolution mechanism. They pointed out that the ionic liquid 1-butyl-3-methylimidazolium chloride (BmimCl) more effectively dissolved CE than its rivals, including BmimBr, BmimSCN and $BmimBF_4$ (Swatloski et al., 2002). This result was proven by NMR method (Remsing, Swatloski, Rogers, & Moyna, 2006).

Similarly, Mantz et al. (Phillips et al., 2004) successfully prepared SF solutions, together with regenerated films using methanol and acetonitrile as the coagulants. Zhang et al. (Xie, Li, & Zhang, 2005) reported that wool keratin (WK) could also be dissolved in BmimCl ionic liquid. As a result, WK/CE blend films were obtained, which opened up an unexplored frontier for preparing bio-base blend films with ionic liquids.

Among versatile designable and functional ionic liquids, BmimCl is easily obtained and high effectively dissolves biopolymers. Here, BmimCl is selected as the solvent for directly dissolving SF and CE. To avoid the re-dissolution of SF and CE during the regeneration process, the right selection and application of coagulation agents would be the main challenge in preparing SF/CE blend films with ionic liquids. In general, the BmimCl ionic liquid can be miscible with water or methanol. Due to the re-dissolution of SF in water while crystallisation of SF induced by methanol (Jin et al., 2005; Phillips et al., 2005), herein, methanol is selected as the coagulation agent.

To date, there is little literature available on the fabrication of SF/CE blend films using ionic liquids. Therefore, we prepared the SF/CE blend films by applying the BmimCl ionic liquid as the solvent and focused on the physical properties of the resulting blend films.

Table 1
The film codes for various blend weight ratios of SF to CE.

Film codes	SF (wt%)	CE (wt%)
SC100	100	0
SC75	75	25
SC50	50	50
SC25	25	75
SC0	0	100

2. Experiment

2.1. Materials

Silk cocoon (*Bombix mori*) was degummed with 0.5% (w/w) aqueous Na_2CO_3 solution at 100 °C for 60 min, washed with water and dried in vacuum at 40 °C for 24 h. The white SF was obtained and coded as SF. Microcrystalline CE powder (Sigma–Aldrich, USA) was coded as CE and used without further treatment. The commercial ionic liquid BmimCl (purity ≥ 99%) (Shanghai Cheng Jie Chemical Co. Ltd.) was also directly applied without further treatment. All other chemicals were of analytical grade.

2.1.1. Preparation of blend films

SF and CE were dispersed separately into 20 g molten BmimCl in a 50 mL flask. The SF-BmimCl and CE-BmimCl solutions were heated at 90 °C with continuous stirring until the clear and viscous solutions were obtained, confirmed by an optical microscope (Fig. 1). The concentration of each solution was calculated to be approximately 2 wt%. The obtained solutions were mixed to produce blend solutions having designed SF to CE weight ratios of 75:25, 50:50 and 25:75. The blend solutions were further stirred for 12 h at 90 °C to ensure the complete intermixing. The resulted SF/CE BmimCl solution was dumped slowly into the polystyrene dishes and kept at 20 °C for 24 h. Then, methanol was slowly added into the dishes; it covered the blend surface and remained in the dishes for another 24 h. The precipitated SF/CE blend films were continuously washed with DI water until complete removal of BmimCl was confirmed with the $AgNO_3$ solution. The gel-like materials were dried at 20 °C for 3 days. The film codes are listed in Table 1. For comparison, the pure SF film and pure CE film were prepared using

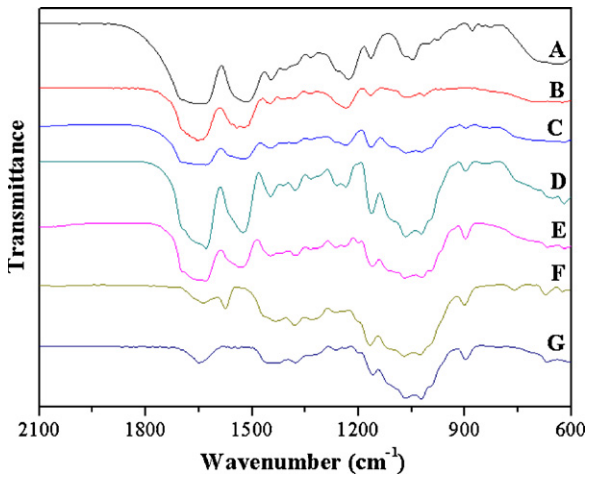

Fig. 2. FTIR spectra of the blend films. (A) Pure SF film washed with methanol, (B) SC100, (C) SC75, (D) SC50, (E) SC25, (F) SC0 and (G) pure CE film washed with methanol.

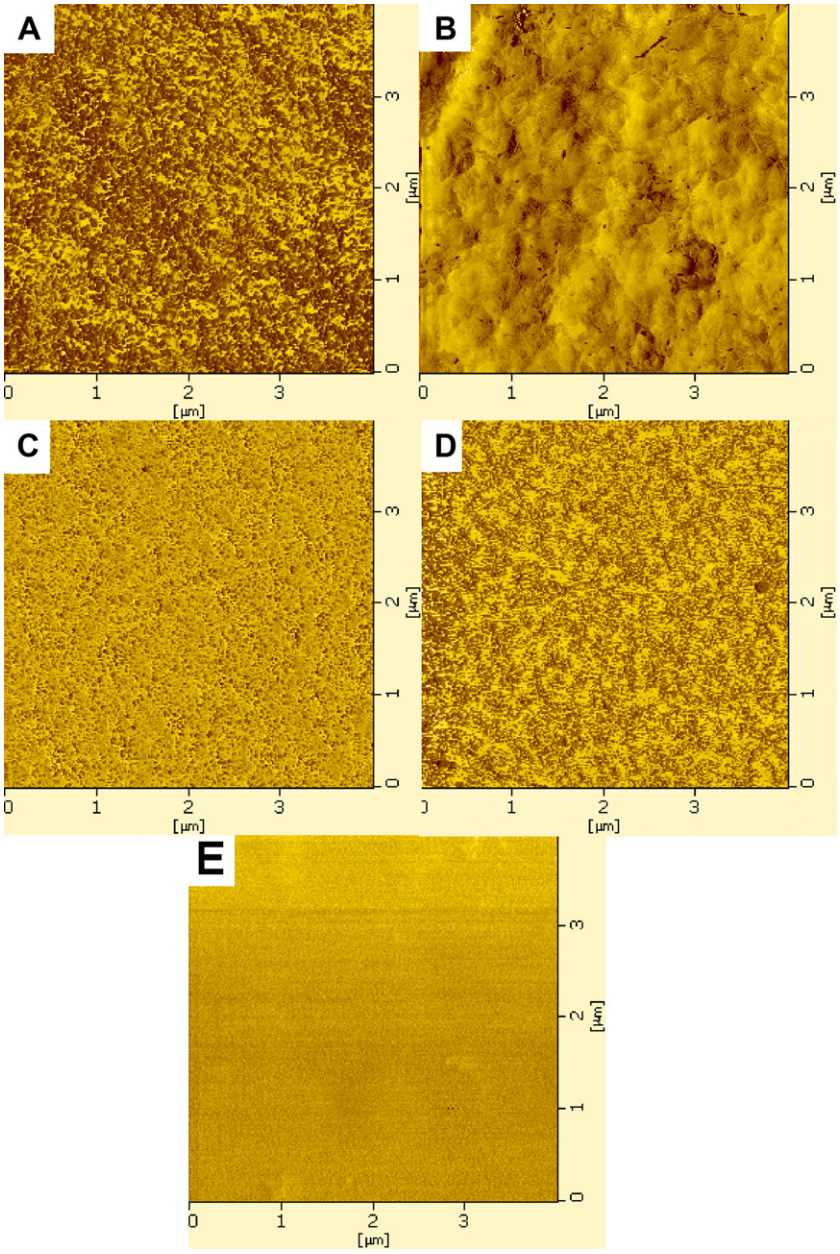

Fig. 3. AFM phase images of the blend films. (A) SC100, (B) SC75, (C) SC50, (D) SC25 and (E) SC0. Each image is 4 μm × 4 μm.

methanol as coagulant and washing agent, followed by the same method for that of the SF/CE blend films.

2.2. Characteristics of the blend films

Fourier transform infrared spectra (FTIR) of the blend films were recorded by a Perkin Elmer 100 (USA) spectrophotometer using the KBr disc technique, in the range 4000–500 cm^{-1} and with a resolution of 0.09 cm^{-1} by using 4× scans per sample.

The surface morphology of the blend films was characterised by a scanning probe microscopy system (Seiko SPI4000, Japan) under ambient conditions using tapping mode probes with constant amplitude (200 mV).

Thermogravimetric (TG) measurements were performed by means of a Netzch 449 C TGA/DSC analyser (Germany) from the temperature 30–500 °C, and the samples were preheated at 100 °C for 10 min to induce dehydration before measurements. All the measurements were carried out under a nitrogen atmosphere at a heating rate of 10 °C/min.

The blend films were placed in a conditioned room (20 °C, 65% RH) for 24 h before testing. The tensile stress and elongation at break of the samples were measured on a universal testing machine (Instron 4411) according to ISO 6239 at a tensile rate of 10 mm/min in the conditioned room (20 °C, 65% RH). The reported values were the average of three measurements.

Moisture content (MC) of the blend films was determined by the following method. Briefly, the samples (10 mm × 10 mm) were conditioned under standard conditions (20 °C, 65% RH) for 24 h before weighing (W_c). The same films were then dried in an oven at 105 °C for 4 h before weighing (W_d). The moisture content was an average of three different determinations, and it was calculated as follows:

$$MC = \frac{W_c - W_d}{W_c} \times 100\% \quad (1)$$

where W_c and W_d are the conditioned and dried weight of the films, respectively.

Films were cut into pieces (10 mm × 10 mm) and dried in the oven at 105 °C for 4 h before weighing (W_0). Several of the same films were then immersed in 100 mL distilled water at 20 °C. Samples were then removed after 10 min, 30 min, 60 min, 120 min and 240 min, respectively. The surface water of the samples was wiped off before they were weighed (W_s). After that, the films were dried at 105 °C for 4 h to determine the final dried weight (W_f). Swelling index (SI), total water absorption (TWA) and film weight loss (FWL) were the averages of three measurements; they were calculated from the following equations:

$$SI = \frac{W_s - W_0}{W_s} \times 100\% \quad (2)$$

$$TWA = \frac{W_s - W_f}{W_s} \times 100\% \quad (3)$$

$$FWL = \frac{W_0 - W_f}{W_0} \times 100\% \quad (4)$$

where W_0, W_s and W_f represent the dried weight of the film before swelling, the swollen weight of the film and the final dried weight of the film after swelling, respectively.

2.3. Statistical analysis

Data from the above experiments are expressed as mean ± standard error of the mean. Statistical analysis was conducted by ANOVA with Student's t test using the Minitab v. 14 statistical package (Minitab Inc., PA, USA). In all statistical evaluations, $p < 0.05$ were considered to be statistically significant, shown with *, while $p < 0.01$ was considered to be especially significant, shown with **.

3. Results and discussion

To investigate the conformational characterisation in the polymer matrix, FTIR spectroscopy measurements were performed. It is reported that the characteristic absorption bands of SF appear at 1630 cm^{-1} (amide I), 1530 cm^{-1} (amide II) and 1260 cm^{-1} (amide III) are assigned to the crystalline β-sheet structure, while the bands at 1660 cm^{-1} (amide I), 1540 cm^{-1} (amide II) and 1230 cm^{-1} (amide II) are attributed to the random coil form or silk I (Freddi et al., 1995). As seen from Fig. 2, the characteristic absorption bands of SC100, attributed to random coil form or silk I, appeared at 1654, 1540 and 1234 cm^{-1}. For comparison, the pure SF film washed with methanol presented the predominant β-sheet structure. On the other hand, the characteristic absorption bands of SC0 appeared 1374, 1161, 1070 and 899 cm^{-1}, which were attributed to the typical amorphous structure of cellulose (Kondo & Sawatari, 1996); similar to that of pure CE film washed with methanol. It is noted that with the increase of CE, the characteristic absorption bands of the blend films at 1654 and 1540 cm^{-1} disappeared with the decreasing intensity at 1234 cm^{-1}. Simultaneously, the amide I band of the blend films shifted to higher wavenumber, from 1624 cm^{-1} for SC75 to 1630 cm^{-1} for SC25, together with the increased intensity at 1265 cm^{-1}. This result indicates that the strong interactions (such as hydrogen bonds) between SF and CE induced the conformational transition of SF from random coil form or silk I to β-sheet structure (Yang et al., 2000). Among them, the strongest interactions between SF and CE appeared in SC25, which could be further proven. The above results can be interpreted as follows: due to the metastable state (Fossey et al., 1991; Chen et al., 2001) of silk I structure obtained by air-drying method and the more stable state of β-sheet structure, the intrinsic tendency towards the state with lower conformation energy is very strong. Under some environmental stimulation, such as blending with polyhydroxyl macromolecules (Freddi et al., 1995) or treating with low dielectric constant organic solvents (Phillips et al., 2004), the interactions between SF and CE may promote and stabilize the ordered β-sheet structure to lower the conformation energy, resulting in the conformation transition of SF (Zhou et al., 2004).

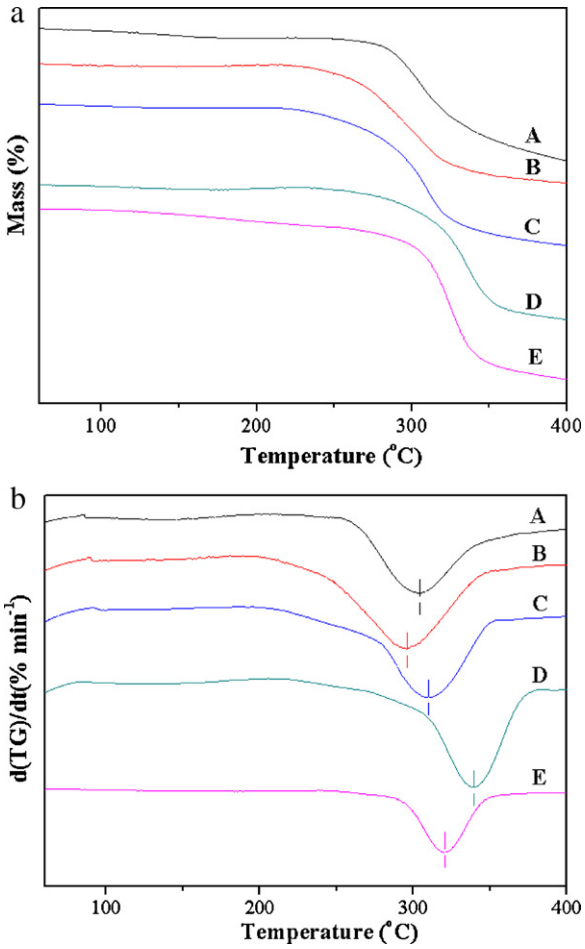

Fig. 4. TG and DTG curves of the blend films. (A) SC100, (B) SC75, (C) SC50, (D) SC25 and (E) SC0.

Investigation of the surface morphology of the blend films was conducted using atomic force microscopy (AFM). Fig. 3 demonstrates that the surface morphology of the blend films varied significantly with CE content. SC100 exhibited a nearly homogeneous surface while the surface morphology of SC75 changed significantly and became heterogeneous with the slightly separated SF/CE phase interface. The SF-rich phase and the CE-rich phase in SC75, however, cannot be easily distinguished in Fig. 3, which was similar to the results obtained by Guo (Hameed & Guo, 2009). This similarity could be due to the insufficient interactions between SF and CE in SC75. With increased CE content, however, the surface morphology of the blend films became more homogeneous and the compatibility was improved. It is worth noting that when CE content was controlled at 75 wt% for SC25, the blend film should result in a heterogeneous surface, similar to that of SC75. It was the very strong interactions between SF and CE component, however, that made the real surface appear much more homogeneous.

To investigate the thermal stability of the blend films, the analysis of thermogravimetric (TG) and derivative thermogravimetric (DTG) was carried out. The blend films only showed a one-step degradation process, illustrated in Fig. 4a. While heating from 50 °C to the initial degradation temperature, the mass loss of

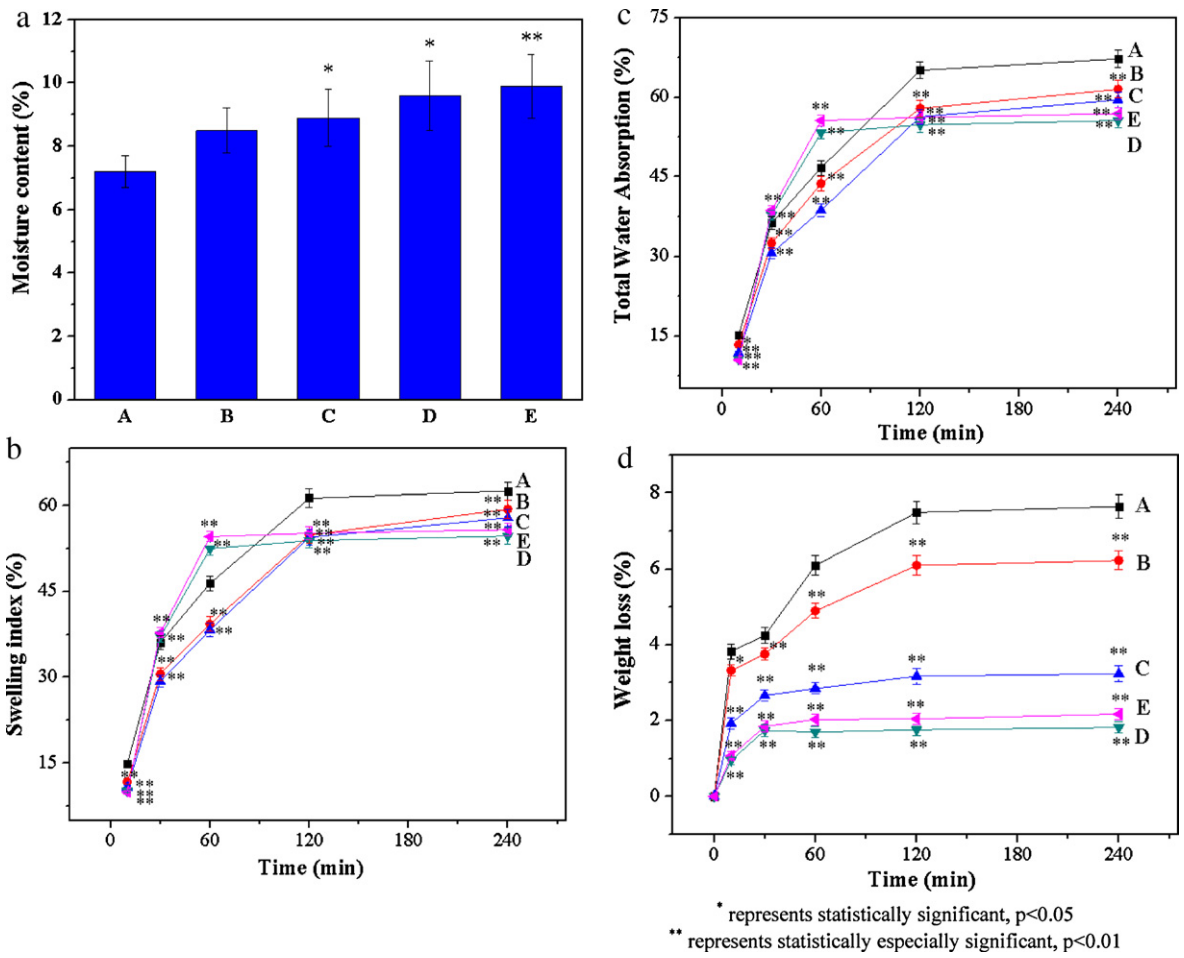

Fig. 5. Moisture content (a), swelling index (b), total water absorption (c) and weight loss (d) of the blend films. (A) SC100, (B) SC75, (C) SC50, (D) SC25 and (E) SC0.

SC100 increased steadily, perhaps due to the changes in amorphous regions of SF. From the onset temperature of degradation the mass loss rate increased and attained its maximum at 303 °C (Fig. 4b), corresponding to the degradation of the polymer matrix. During further heating, the degradation rate slowed down. Similar to the degradation process of SF, the mass loss of CE increased gradually before the onset temperature of degradation. The mass loss rate then increased and reached its maximum at 319 °C (Fig. 4b), corresponding to the degradation of the polymer matrix. It is clear that the maximum mass loss rate of SF appeared at 303 °C, lower than that of CE, which is similar to the results of Sashina, Janowska, Zaborski, & Vnuchkin (2007). This result could be because the interactions in the amorphous sections of SF are much weaker than such interactions in the amorphous sections of CE. When the temperature increased, fewer interactions in SF matrix could prevent its degradation, while the more interactions in CE matrix could prevent an ordered structure formation in certain segments and contribute to the higher temperature of maximum mass loss rate. Different with the initial mass loss curves of SF and CE, until the onset temperature of degradation, the other blend films retained most of their mass. When the content of CE in the blend films increased, the maximum mass loss rate of the samples appeared at higher temperature. The blend film SC75 showed the lower temperature of maximum mass loss rate than that of SF, which could be due to the bad compatibility between SF and CE component. On the other hand, the strongest interactions took place in SC25, contributing to the highest temperature of maximum mass loss rate.

Mechanical properties are one of the important factors for assessing the application of the blend films. Table 2 provides information on the varied tensile strength and elongation at break by changing the SF/CE blend component. With increasing CE content, the tensile strength significantly rose (except for SC75) and reached a maximum when the CE content remained at 75 wt%. The improved tensile strength of the blend films could be due to the strong interactions between SF and CE and corresponding increased β-sheet structure (Marsano, Corsini, Canetti, & Freddi, 2008). When CE was added to SF, more tensile force was required to break the film. However, due to the insufficient interactions and bad compatibility between SF and CE in SC75, the increase in tensile strength was only 20%, compared with SC100. When the CE content accounted for 50 wt%, the value of tensile strength was double that of SF. When the CE content was 75 wt%, the highest increase of tensile strength was achieved. On the other hand, compared with

Table 2
Mechanical properties of the blend films.

Sample	Tensile strength (MPa)	Elongation at break (%)
SC100	4.2 ± 0.6	46.3 ± 5.8
SC75	5.3 ± 0.9	50.5 ± 4.9
SC50	8.5 ± 1.1**	60.3 ± 6.1*
SC25	13.1 ± 1.4**	52.8 ± 5.7
SC0	11.5 ± 1.1**	54.7 ± 5.2

* Statistically significant, $p < 0.05$.
** Statistically significant, $p < 0.01$.

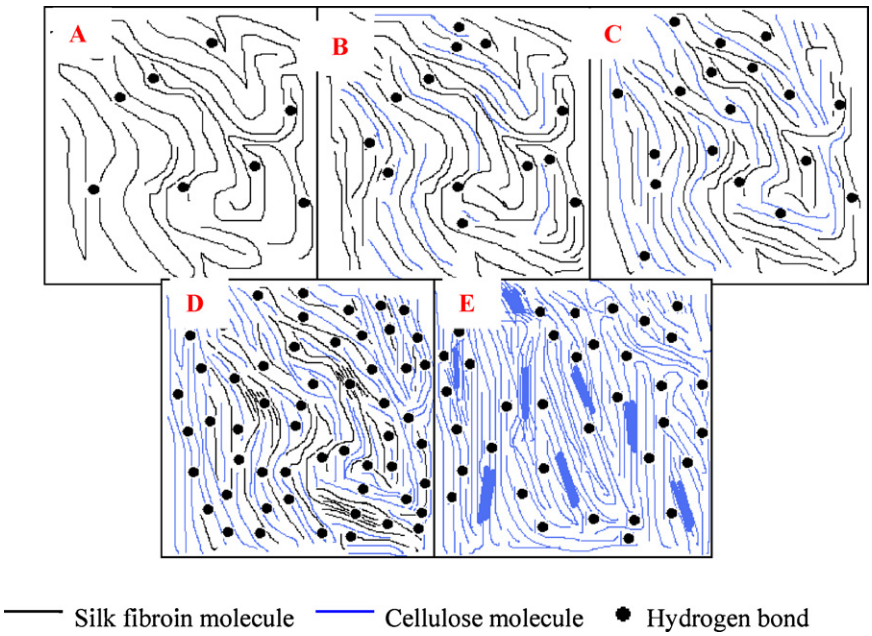

Fig. 6. Schematic model proposed for the blend films. (A) SC100, (B) SC75, (C) SC50, (D) SC25 and (E) SC0.

that of SF, the elongation at break of the blend films displays the initial ascent trend when CE content increased to 50 wt%, then took a rapid drop for 75 wt% CE content and finally rose again for CE. Such observations were slightly different with the results of tensile strength of the blend films. This result could be because SC50 had desirable proportion and excellent compatibility between SF and CE, contributing to the higher elongation at break.

Moisture content reflects the surface hydrophilicity, which could be affected by both the hydrophilic nature and the surface roughness. Fig. 5a illustrates the increasing tendency of moisture content with more CE content in the blend films. The results indicated that SC100 had the lowest surface hydrophilicity due to its lowest moisture content. When 25 wt% CE was added to SF, the moisture content increased sharply due to the introduction of the more hydrophilic CE. However, there was a small increase in moisture content of SC50 due to the more homogeneous surface of the film, which could be confirmed from AFM observations. It is also interesting to note that SC0 had slightly higher moisture content than SC25 due to the more homogeneous surface. The values of moisture content here were slightly lower than those reported by Freddi et al. (1995), which could be explained by the washing process. The glycerine–water solution most likely promoted the higher moisture content of the blend films.

Swelling index and total water absorption can reflect the interactions, including surface and internal regions of the film and water. If the film dissolves well in water, the difference between swelling index and total water absorption could not be ignored. Here, the swelling index and total water absorption of the blend films are shown in Fig. 5b and c. The following observations were made: (1) swelling index in value was slightly lower than that of total water absorption, which was more apparent when the immersion time was longer. (2) Various blend films had different equilibrium time, for example, SC100 had the longest equilibrium time (120 min) while SC25 and SC0 had the shortest equilibrium time (60 min) both for swelling index and total water absorption. (3) With the increase of CE, the swelling index and total water absorption of the blend films significantly decreased. SC100 had the highest values of swelling index and total water absorption, whereas SC25 had the lowest values under the same conditions. The above results can be interpreted as follows: when blend films were immersed in water, the water molecules would approach the hydrophilic region and bind the blend films, while the interactions in the film and the resulting increased β-sheet structure would prevent the binding of water. With the increase of CE, the greater effect of inhibiting the binding of water than the effect of promoting the swelling of blend films led to lower swell index and total water absorption.

SF films with dominating amorphous structures were easily soluble in water (Lu et al., 2010), and many attempts were made to increase the insolubility of the film by conformational transition (Hu, Kaplan, & Cebe, 2008; Tsukada et al., 1994). The weight loss of these films in water for various periods is shown in Fig. 5d. Comparison of the film weight loss led to the following observations. (1) Various blend films had different equilibrium time, SC100 had the longest equilibrium time (120 min) while SC25 and SC0 had the shortest (30 min). (2) With increasing CE, the weight loss of the blend films significantly decreased. SC25 was almost undissolved in water for 240 min, whereas there was about 8% weight loss under the same conditions for SC100. These results are consistent with those of swelling behavior, indicating that SC25 possesses more excellent water stability in this study.

Based on the above discussion, a model for such blend films is proposed, as illustrated in Fig. 6. Under the present conditions, SC100 has the weakest intermolecular interactions in the matrix while SC25 has the strongest interactions in the matrix.

4. Conclusions

Introduction of CE into SF has induced the conformation transition of SF from random coil form or silk I to β-sheet structure. Compared with the pure SF film, the physical properties of the blend films are improved with incorporation of CE. When the ratio of SF to CE is 25:75, the blend film illustrates the higher tensile strength, higher thermal stability and higher water stability due to strong interactions in the matrices. However, the blend film with half CE exhibits more homogeneous surface and higher miscibility. Our work has demonstrated a good example of the preparation of SF/CE blend films regenerated from BmimCl ionic liquid. It can be expected that the blend films with improved physical properties may play an important role in biochemical and biomedical applications.

Acknowledgements

The authors would like to acknowledge the Research Committee of The Hong Kong Polytechnic University for the provision of a scholarship to Lei Zhu. The authors would also like to express their gratitude to all the reviewers for their helpful comments and suggestions.

References

Atsumi, S., Hanai, T., & Liao, J. C. (2008). Non-fermentative pathways for synthesis of branched-chain higher alcohols as biofuels. *Nature*, *451*, 86–89.

Chen, X., Shao, Z. Z., Marinkovic, N. S., Miller, L. M., Zhou, P., & Chance, M. R. (2001). Conformation transition kinetics of regenerated *Bombyx mori* silk fibroin membrane monitored by time-resolved FTIR spectroscopy. *Biophysical Chemistry*, *89*, 25–34.

Fernandes, S. C. M., Oliveira, L., Freire, C. S. R., Silvestre, A. J. D., Neto, C. P., Gandini, A., et al. (2009). Novel transparent nanocomposite films based on chitosan and bacterial cellulose. *Green Chemistry*, *11*, 2023–2029.

Fossey, S. A., Nemethy, G., Gibson, K. D., & Scheraga, H. A. (1991). Conformational energy studies of beta-sheets of model silk fibroin peptides. I. Sheets of poly(ala-gly) chains. *Biopolymers*, *31*, 1529–1541.

Freddi, G., Pessina, G., & Tsukadab, M. (1999). Swelling and dissolution of silk fibroin (*Bombyx mori*) in N-methyl morpholine N-oxide. *International Journal of Biological Macromolecules*, *24*, 251–263.

Freddi, G., Romano, M., Massafra, M. R., & Tsukada, M. (1995). Silk fibroin/cellulose blend films – preparation, structure, and physical-properties. *Journal of Applied Polymer Science*, *56*, 1537–1545.

Gupta, M. K., Khokhar, S. K., Phillips, D. M., Sowards, L. A., Drummy, L. F., Kadakia, M. P., et al. (2007). Patterned silk films cast from ionic liquid solubilized fibroin as scaffolds for cell growth. *Langmuir*, *23*, 1315–1319.

Hameed, N., & Guo, Q. P. (2009). Natural wool/cellulose acetate blends regenerated from the ionic liquid 1-butyl-3-methylimidazolium chloride. *Carbohydrate Polymers*, *78*, 999–1004.

Hu, X., Kaplan, D., & Cebe, P. (2008). Dynamic protein–water relationships during β-sheet formation. *Macromolecules*, *41*, 3939–3948.

Jin, H. J., Park, J., Karageorgiou, V., Kim, U. J., Valluzzi, R., Cebe, P., et al. (2005). Water-stable silk films with reduced beta-sheet. *Advanced Functional Materials*, *15*, 1241–1247.

Kaplan, D., Adams, W. W., Farmer, B., & Viney, C. (Eds.). (1994). *ACS symposium series 544 Silk polymers: Materials science and biotechnology*. Washington, DC: American Chemical Society.

Kondo, T., & Sawatari, C. (1996). A Fourier transform infra-red spectroscopic analysis of the character of hydrogen bonds in amorphous cellulose. *Polymer*, *37*, 393–399.

Kweon, H., Ha, H. C., Um, I. C., & Park, Y. H. (2001). Physical properties of SF/chitosan blend films. *Journal of Applied Polymer Science*, *80*, 928–934.

Lawrence, B. D., Marchant, J. K., Pindrus, M. A., Omenetto, F. G., & Kaplan, D. L. (2009). Silk film biomaterials for cornea tissue engineering. *Biomaterials*, *30*, 1299–1308.

Lawrence, B. D., Omenetto, F., Chui, K., & Kaplan, D. L. (2008). Processing methods to control SF film biomaterial features. *Journal of Materials Science*, *43*, 6967–6985.

Li, M. Z., Minoura, N., Dai, L. X., & Zhang, L. S. (2001). Preparation of porous poly(vinyl alcohol)–SF (PVA/SF) blend membranes. *Macromolecular Materials and Engineering*, *286*, 529–534.

Li, W. Y., Jin, A. X., Liu, C. F., Sun, R. C., Zhang, A. P., & Kennedy, J. F. (2009). Homogeneous modification of cellulose with succinic anhydride in ionic liquid using 4-dimethylaminopyridine as a catalyst. *Carbohydrate Polymers*, *78*, 389–395.

Lu, J., Wang, T., & Drzal, L. T. (2008). Preparation and properties of microfibrillated cellulose polyvinyl alcohol composite materials. *Composites Part A-Applied Science and Manufacturing*, *39*, 738–746.

Lu, S. Z., Wang, X. Q., Lu, Q., Hu, X., Uppal, N., Omenetto, F. G., et al. (2009). Stabilization of enzymes in silk films. *Biomacromolecules*, *10*, 1032–1042.

Lu, S. Z., Wang, X. Q., Lu, Q., Zhang, X. H., Kluge, J. A., Uppal, N., et al. (2010). Insoluble and flexible silk films containing glycerol. *Biomacromolecules*, *11*, 143–150.

Ma, X. F., & Yu, J. G. (2004). The plastcizers containing amide groups for thermoplastic starch. *Carbohydrate Polymers*, *57*, 197–203.

Marsano, E., Corsini, P., Canetti, M., & Freddi, G. (2008). Regenerated cellulose–silk fibroin blends fibers. *International Journal of Biological Macromolecules*, *43*, 106–114.

Niamsa, N., Srisuwan, Y., Baimark, Y., Phinyocheep, P., & Kittipoom, S. (2009). Preparation of nanocomposite chitosan/SF blend films containing nanopore structures. *Carbohydrate Polymers*, *78*, 60–65.

Phillips, D. M., Drummy, L. F., Conrady, D. G., Fox, D. M., Naik, R. R., Stone, M. O., et al. (2004). Dissolution and regeneration of *Bombyx mori* silk fibroin using ionic liquids. *Journal of the American Chemical Society*, *126*, 14350–14351.

Phillips, D. M., Drummy, L. F., Naik, R. R., De Long, H. C., Fox, D. M., Trulove, P. C., et al. (2005). Regenerated silk fiber wet spinning from an ionic liquid solution. *Journal of Materials Chemistry*, *15*, 4206–4208.

Remsing, R. C., Swatloski, R. P., Rogers, R. D., & Moyna, G. (2006). Mechanism of cellulose dissolution in the ionic liquid 1-n-butyl-3-methylimidazolium chloride: a C-13 and Cl-35/37 NMR relaxation study on model systems. *Chemical Communications*, *12*, 1271–1273.

Rubin, E. M. (2008). Genomics of cellulosic biofuels. *Nature*, *454*, 841–845.

Sashina, E. S., Janowska, G., Zaborski, M., & Vnuchkin, A. V. (2007). Compatibility of fibroin/chitosan and fibroin/cellulose blends studied by thermal analysis. *Journal of Thermal Analysis and Calorimetry*, *89*, 887–891.

Swatloski, R. P., Spear, S. K., Holbrey, J. D., & Rogers, R. D. (2002). Dissolution of cellose with ionic liquids. *Journal of the American Chemical Society*, *124*, 4974–4975.

Tsukada, M., Cotoh, Y., Nacura, M., Minoura, N., Kasai, N., & Freddi, C. (1994). Structural changes of silk fibroin membranes induced by immersion in methanol aqueous solutions. *Journal of Polymer Science Part B: Polymer Physics*, *32*, 961–968.

Vepari, C., & Kaplan, D. L. (2007). Silk as a biomaterial. *Progress in Polymer Science*, *32*, 991–1007.

Wang, Y. Z., Kim, H. J., Novakovic, G. V., & Kaplan, D. L. (2006). Stem cell-based tissue engineering with silk biomaterials. *Biomaterials*, *27*, 6064–6082.

Xie, H. B., Li, S. H., & Zhang, S. B. (2005). Ionic liquids as novel solvents for the dissolution and blending of wool keratin fibers. *Green Chemistry*, *7*, 606–608.

Yang, G., Zhang, L. N., & Liu, Y. G. (2000). Structure and microporous formation of cellulose/silk fibroin blend membranes: I. Effect of coagulants. *Journal of Membrane Science*, *177*, 153–161.

Yang, Q. L., Lue, A., Qi, H. S., Sun, Y. X., Zhang, X. Z., & Zhang, L. N. (2009). Properties and bioapplications of blended cellulose and corn protein films. *Macromolecular Bioscience*, *9*, 849–856.

Zhang, Y. Q. (1998). Natural silk fibroin as a support for enzyme immobilization. *Biotechnology Advances*, *16*, 961–971.

Zhang, H., Wang, Z. G., Zhang, Z. N., Wu, J., Zhang, J., & He, H. S. (2007). Regenerated-cellulose/multiwalled-carbon-nanotube composite fibers with enhanced mechanical properties prepared with the ionic liquid 1-allyl-3-methylimidazolium chloride. *Advanced Materials*, *19*, 698–704.

Zhou, P., Xie, X., Deng, F., Ping, Z., Xun, X., & Feng, D. (2004). Effects of pH and calcium ions on the conformational transitions in silk fibroin using 2D Raman correlation spectroscopy and C-13 solid-state NMR. *Biochemistry*, *43*, 11302–11311.

Zhu, S. D., Wu, Y. X., Chen, Q. M., Yu, Z. N., Wang, C. W., Jin, S. W., et al. (2006). Dissolution of cellulose with ionic liquids and its application: A mini-review. *Green Chemistry*, *8*, 325–327.